Polarization Dependent Four-Wave-Mixing and Two-Photon Coherence in Solids

M. Sheik-Bahae, *Member, IEEE*, J. Wang, E. J. Canto-Said, R. DeSalvo, D. J. Hagan, *Member, IEEE*, and E. W. VanStryland, *Senior Member, IEEE*

Abstract — **Polarization dependent degenerate-four-wave-mixing experiments on semiconductors (ZnSe, CdS) and dielectrics (NaCl, PbF_2) reveal the essential mechanisms of the bound-electronic $\chi^{(3)}$. We show, for the first time, that the observed anomalous dispersion of the polarization dependent phase-conjugate reflectivity can be explained using a simple 3-band model. The near vanishing reflectivity in the two-photon coherence geometry is shown to be a consequence of the interference between transitions originating from heavy- and light-hole valence bands. We also present measurements on the polarization dichroism of the nonlinear refractive index (n_2), in good agreement with this simple theory.**

POLARIZATION dependent optical nonlinearities have been subject to numerous experimental and theoretical investigations for many years [1]–[6]. Using techniques ranging from nonlinear transmission to four-wave-mixing, experiments have been conducted to unveil information on the structural symmetry of nonlinear materials. In solids, such information pertains to the crystal symmetry and the details of the band structure. In the case of resonant excitation where electron-hole pairs are generated, degenerate-four-wave-mixing (DFWM) has been employed to study the carrier dynamics (diffusion) and anisotropic state-filling [3], [5]. With excitation in the transparency region of solids, however, the nonlinear polarization arises from the anharmonic response of valence electrons, and is characterized by the nearly instantaneous third-order susceptibility $\chi^{(3)}$. The tensor elements of $\chi^{(3)}$, and particularly the anisotropy of the two-photon absorption (2PA) coefficient, have been previously investigated theoretically and experimentally for a variety of crystalline structures [6], [7]. From a practical point of view, it is essential to understand the polarization dependence of optical nonlinearities for all-optical switching devices in which, for example, the control and signal pulses do not possess the same polarization.

Manuscript received September 28, 1994; revised February 6, 1995. This work was supported by the National Science Foundation Grant ECS#9120590, the Advanced Projects Agency, and the Naval Air Warfare Center Joint Service Agile Program Contract N66269-C-93-0256.

M. Sheik-Bahae is with the Department of Physics and Astronomy, University of New Mexico, Albuquerque, NM 87131 USA.

J. Wang with the Advanced Technology Research & Development Division, Hitachi Ltd., Kanagawa-ken 256, Japan.

E. J. Canto-Said, D. J. Hagan, and E. W. VanStryland are with the Center for Research and Education in Optics and Lasers, Departments of Physics and Electrical Engineering, University of Central Florida, Orlando, FL 32816 USA.

R. DeSalvo is with the Information System Division, Harris Corporation, Melbourne, FL 32902 USA.

IEEE Log Number 9411892.

Here, we report the polarization dependence of the DFWM signal for a number of polycrystalline (i.e., macroscopically isotropic) solids. We show that the observed wavelength dispersion in the induced anisotropy can be explained in terms of additive contributions from two valence bands having symmetries of heavy and light-hole valence bands described by the Kane model [8]. The experimental configuration is a standard backward phase-conjugate DFWM geometry in which two pump beams E_f (forward) and E_b (backward), and a probe beam E_p, propagating at a small angle to the forward pump, interact in the nonlinear medium to generate the phase-conjugate beam E_c, retro-reflected along the direction of the probe [1]. The dependence of the phase-conjugate signal on the polarization of the incident beams can be written in terms of vector inner products of the interacting electric fields [2]:

$$\vec{E}_c \propto A\vec{E}_f(\vec{E}_b\cdot\vec{E}_p^*)+B\vec{E}_b(\vec{E}_f\cdot\vec{E}_p^*)+C\vec{E}_p^*(\vec{E}_b\cdot\vec{E}_f). \quad (1)$$

The three polarization combinations are described as follows. a) $E_f \perp E_p \| E_b$. This is known as the small period grating since the interference of E_p and E_b results in a spatial grating that scatters E_f into the conjugate direction. The grating period is termed "small" because of the large angle between the wave-vectors of the interfering fields E_p and E_b. The relative strength of E_c, in this case, is determined by the A coefficient, or $|A|^2$ for the phase-conjugate reflectivity. b) $E_b \perp E_p \| E_f$. This geometry also leads to a spatial grating which, due to the small angle of the interfering fields, is referred to as the large period grating. The phase conjugate reflectivity is proportional to $|B|^2$. c) $E_p \perp E_f \| E_b$. Here the interference of the two counter-propagating pump beams gives rise to a temporal grating oscillating at twice the optical frequency ω. This has been termed as the two-photon coherence (or 2ω-coherence) term. The phase conjugate reflectivity for this configuration is proportional to $|C|^2$. In all three cases, there exist implicitly additional grating terms that result from the interaction of two cross-polarized fields producing a polarization grating that scatters the third beam. Finally, with all beams co-polarized, the relative reflectivity is given by $|A+B+C|^2$.

It has been widely believed that the 2ω-coherence term must be small unless near a 2PA resonance [1], [2]. Our experiments on semiconductors show just the opposite. The 2ω-coherence signal is large unless we are in the 2PA resonant regime where the signal nearly vanishes. In this letter we explain this behavior as the interference of the contributions from light-hole and heavy hole valence bands.

TABLE I
THE NORMALIZED PHASE CONJUGATE AMPLITUDES MEASURED USING POLARIZATION SELECTIVE DFWM WITH PICOSECOND PULSES AT $\lambda = 532$ nm

	NaCl	*PbF_2*	*ZnSe*	*CdS*
|A+B+C|	1	1	1	1
|B|	0.34	0.41	0.57	0.58
|C|	0.31	0.34	0.08	0.05

We performed experiments with ZnSe, CdS, PbF_2 and NaCl using 20 picosecond pulses from a Q-switched, modelocked, frequency doubled Nd:YAG laser having a wavelength (λ) of 532 nm. These materials were selected to provide a range of $\hbar\omega/E_g$ (where $\hbar\omega$=photon energy and E_g=energy band-gap) that spanned from near resonance ($\hbar\omega/E_g \approx 1$) to below the 2PA region ($\hbar\omega/E_g < 0.5$). The DFWM experimental results are summarized in Table I where we list the phase-conjugate amplitudes $|B|$ and $|C|$, normalized to $|A+B+C| = 1$. For ZnSe with $E_g \cong 2.6$ eV and CdS with $E_g \cong 2.4$ eV, 2PA is allowed, making $\chi^{(3)}$ complex (i.e., $\Im m\{\chi^{(3)}\} \neq 0$). As was shown in [4], in addition to the bound-electronic $\chi^{(3)}$, which appears instantaneously in a time-resolved study, 2PA-generated charge carriers also contribute to the observed signal but decay by diffusion of carriers across the grating period. In that case, the pure $\chi^{(3)}$ contributions can be separated from the free carrier effects by their longer decay time and realizing that the effective nonlinearity due to 2PA-generated carriers is of higher order (i.e., $\chi^{(5)}$). In our experiments, the diffusion time across the small period grating (case a)) was within the duration of the laser pulse. This made it difficult to unambiguously extract the $\chi^{(3)}$ contribution for that geometry. Therefore, we have only listed the results of the large period grating in Table I. This does not limit us in any way from analyzing the data, since for ultrafast nonlinearities (i.e., bound-electronic $\chi^{(3)}$) and isotropic materials, the contribution of both grating terms are identical ($A = B$). One important feature of the data in Table I is the vanishing phase conjugate signal in the 2ω-coherence geometry for ZnSe and CdS (case c)), while NaCl and PbF_2 have nearly equal contributions for all geometries. This is in sharp contrast to previous assertions that the 2ω-coherence signal is negligible unless the excitation is near or within a 2PA resonance region [1], [2].

In isotropic (e.g., polycrystalline) or cubic materials the only nonzero $\chi^{(3)}$ tensor elements are χ_{1212}, χ_{1221}, χ_{1122}, and χ_{1111} with subscripts 1 and 2 denoting the transverse polarization directions of x and y. We have omitted the superscript (3) for brevity. The isotropy condition also implies that $\chi_{1111} = \chi_{1212} + \chi_{1221} + \chi_{1122}$ and $\chi_{1212} = \chi_{1221}$, thus reducing the independent elements to just χ_{1122} and χ_{1212}, for any given physical mechanism. Now consider, for instance, the case c) above where $E_f \| E_b \perp E_p$. Writing E_c in terms of the $\chi^{(3)}$ elements, we obtain:

$$E_c(\omega) \propto \chi_{1212}(\omega;\, \omega,\, -\omega,\, \omega) E_c E_p^* E_b + \chi_{1122}(\omega;\, -\omega,\, \omega,\, \omega) E_p^* E_f E_b. \quad (2)$$

Here, we assign physical significance to the ordering of the frequency arguments in each χ term to represent the time-ordering of the quantum mechanical transition sequence. In other words, $\chi(\omega;\, -\omega,\, \omega,\, \omega)$ corresponds to the process of absorption of two photons followed by emission of two photons. The imaginary part of this quantity is related to the 2PA coefficient. Similarly, $\chi(\omega;\, \omega,\, -\omega,\, \omega)$ corresponds to the sum of contributions from Raman and quadratic Stark effects (QSE) in which the four-photon process is an absorption-emission-absorption-emission sequence [9]. In [9], [10], we showed that these three processes (2PA, electronic Raman and QSE) adequately describe the $\chi^{(3)}$ mechanisms associated with a given two-band system. We will omit the frequency arguments for brevity and instead distinguish the various mechanisms by using superscripts 2PA, Raman and QSE. Now, from (1) and (2), we set:

$$C = \chi_{1122}^{2PA} + \chi_{1212}^{\text{Raman}} + \chi_{1212}^{\text{QSE}}. \quad (3)$$

In a similar manner, one obtains:

$$A = B = \chi_{1212}^{2PA} + (\chi_{1212}^{\text{Raman}} + \chi_{1122}^{\text{Raman}})/2 + (\chi_{1212}^{\text{QSE}} + \chi_{1122}^{\text{QSE}})/2. \quad (4)$$

As expected, the sum $A+B+C$ is equal to the sum of χ_{1111}'s of all three mechanisms once we apply the isotropy condition.

The task at hand is to obtain a proper symmetry relationship between the $\chi^{(3)}$ tensor elements, in order to resolve the anomaly of the DFWM data in Table I. We follow the theoretical approach of [9], [10] where the absorptive and refractive components of $\chi^{(3)}$ were calculated using a simple two-parabolic band model. A light-hole type valence band and a conduction band of equal curvature was assumed. The theory first calculated the nondegenerate absorption spectrum ($\Im m\{\chi^{(3)}\}$), associated with 2PA, Raman and QSE, by evaluating the nonlinear transition rate using a dressed-state formalism. The refractive component ($n_2 \propto \Re e\{\chi^{(3)}\}$) is then calculated using a Kramers–Kronig (K–K) transformation of the nonlinear absorption spectrum. The calculated band-gap scaling, magnitude and dispersion of $\chi^{(3)}$ were shown to be in excellent agreement with the experimental results for a large number of semiconductors and dielectrics [9], [10]. However, the polarization dependence of $\chi^{(3)}$, derived from the two-band model, gives $\chi_{1122} = \chi_{1212} = \chi_{1111}/3$ for all three mechanisms at all wavelengths [10]. This implies, from (3) and (4), that $A = B = C$, a result that certainly disagrees with the near band-gap results of ZnSe and CdS of Table I. Here we go one step further and consider a three-band model incorporating heavy-hole (hh) and light-hole (lh) valence bands and a single conduction (c) band that obey the symmetry given by Kane [8]. In the simplest approximation, we take the $\chi^{(3)}$ elements associated with each mechanism as the sum of contributions from hh-c and lh-c band pairs, i.e., $\chi_{\text{total}} = \chi_{\text{hh-c}} + \chi_{\text{lh-c}}$. The significant distinction between these two band pairs is the k-space orientation of the interband momentum matrix elements ($\boldsymbol{p}_{\text{cv}}$) with respect to the electron quasi-momentum ($\hbar\boldsymbol{k}$). In the Kane band structure, the conduction band is S type while the valence bands are P type. The wavefunction of the valence bands can be written as a superposition of

the band-edge Bloch wavefunctions $|X\rangle$, $|Y\rangle$ and $|Z\rangle$. More specifically, the hh valence band is of $|X \pm iY\rangle$ form while the lh band is a superposition of $|X \pm iY\rangle$ and $|Z\rangle$ wave functions [8]. Without loss of generality, taking $\boldsymbol{k}\|z$ causes the $k.p$ coupling between conduction and hh-valence bands to vanish. In this simple formalism, the absence of $k.p$ coupling in hh-c interaction is the reason for the bare electron effective mass of the hh valence band. One simple way to express the net result is to take $\boldsymbol{k}\|\boldsymbol{p_{cv}}$ for the lh-c, and $\boldsymbol{k} \perp \boldsymbol{p_{cv}}$ for the hh-c transitions. It should be noted that although this k-space symmetry is resulted from Kane's 4-band model (or 8-band when considering the spin degeneracy), we ignore the transitions originating from the split-off valence bands. The significance of this k-space symmetry becomes apparent if we examine the expression for the transition rate due to Raman and 2PA [9]:

$$W_{\vec{k}}^{2PA,\,\mathrm{Raman}} \propto \int \left| \frac{(\vec{a}_1 \cdot \vec{p}_{cv})(\vec{a}_2 \cdot \vec{k})}{\omega_1} \pm \frac{(\vec{a}_2 \cdot \vec{p}_{cv})(\vec{a}_1 \cdot \vec{k})}{\omega_2} \right|^2 \cdot \delta(\hbar\omega_1 \pm \hbar\omega_2 - E_{cv})\, d\vec{k}, \quad (5)$$

where unit vectors $\boldsymbol{a}_1$ and $\boldsymbol{a}_2$ represent the polarization of the two optical fields at frequency ω_1 and ω_2 respectively. $E_{cv} = E_{cv} + \hbar^2k^2/2\boldsymbol{m}_{cv}$ is the interband energy of each band-pair with $\boldsymbol{m}_{cv}$ denoting the corresponding reduced electron-hole effective mass. Although we are concerned with the degenerate ($\omega_1 = \omega_2$) case of $\chi^{(3)}$, a nondegenerate nonlinear absorption spectrum, as obtained from (5), is initially required to obtain the refractive part from a K–K transformation. The sequence of transitions in (5) are typical of a two-band model in which a photon is absorbed in an interband transition followed by an absorption (+sign) or emission (−sign) of the second photon in an intra-band process (self-transition). Using the k-space orientation properties of $\boldsymbol{k}$ and $\boldsymbol{p_{cv}}$, (5) leads to distinctly different polarization dependences for the two-band pairs. The detailed derivation of the $\chi^{(3)}$ symmetry, with absorptive part ($\Im m\{\chi^{(3)}\}$) derived from (5), and the refractive part ($n_2 \propto \Re e\{\chi^{(3)}\}$), obtained from the K–K transformation of the imaginary part, is beyond the scope of this letter. Here, we give relations only for $\Im m\{\chi^{(3)}\}$ due to 2PA. For the lh-c case, as was also given in [9], [10], the polarization dependence of the $\Im m\{\chi^{(3)}\}$ follows the $\chi_{1122} = \chi_{1212} = \chi_{1111}/3$ symmetry. This relation holds even for the real part, independent of the optical frequency. For the hh-c system, however, we obtain the following relationship for the degenerate $\Im m\{\chi^{(3)}\}$:

$$\chi_{1212} = \chi_{1221} = \frac{3}{4}\chi_{1111} \quad \text{and} \quad \chi_{1122} = -\frac{1}{2}\chi_{1111}. \quad (6)$$

Such simple relationships do not necessarily hold for $\Re e\{\chi^{(3)}\}$ at all frequencies. This is because the symmetry relations for the nondegenerate $\Im m\{\chi^{(3)}\}$ are frequency dependent, thus leading to a frequency dependent (dispersive) symmetry for the $\Re e\{\chi^{(3)}\}$ as obtained from the K–K transformation. Symmetry relations similar to (6) were also obtained for the 2PA coefficient (associated with the hh-c transition), using a full Kane-band model [11]. Before discussing the symmetry of the QSE contribution, we examine the implications of the symmetry relations of DFWM due to the 2PA contribution only. Consider the $A(=B)$ and C coefficients in (3) and (4). The 2PA contributions from hh-c and lh-c have opposite signs in C, causing the two effects to partially cancel in the 2ω-coherence geometry. For the A term, on the other hand, the 2PA contributions from the two band pairs add, leading to a larger signal. This is in qualitative agreement with the data on semiconductors in the 2PA region as given in Table I.

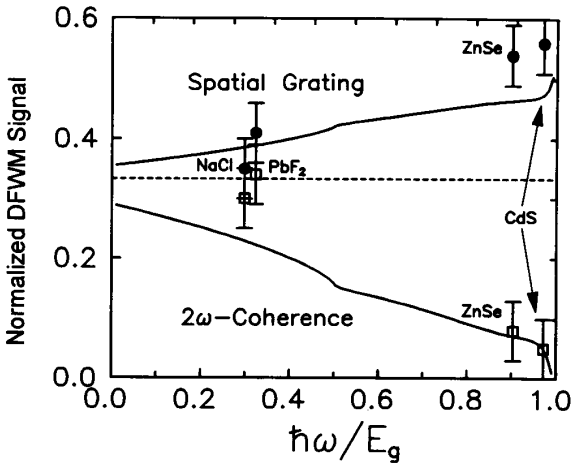

Fig. 1. Data from Table I with solid circles denoting spatial grating terms ($|B|$) while open squares are the $2-\omega$ coherence term ($|C|$). The solid lines are calculated results from the 3-band model while the dashed line represent the 2-band model [9].

The nondegenerate transition rate due to QSE involves only interband transitions:

$$W_{\vec{k}}^{\mathrm{QSE}} \propto \int |(\vec{a}_1 \cdot \vec{p}_{cv})(\vec{a}_2 \cdot \vec{p}_{cv})|^2 \delta(\hbar\omega_1 - E_{cv})\, d\vec{k}. \quad (7)$$

The lack of self-transitions makes the symmetry relations for χ^{QSE} the same for both band pairs, i.e., $\chi_{1122} = \chi_{1212} = \chi_{1111}/3$ (for real and imaginary parts) independent of optical frequency.

In adding up all the contributions of the two band-pairs for both refractive and absorptive processes, we obtain the complex coefficients A, B, and C as a function of $\hbar\omega/E_g$. In order to compare the results with the data in Table I, we evaluate $|A|$, $|B|$, and $|C|$, normalized with respect to $|A + B + C|$ corresponding to the case of all co-polarized beams. This comparison is shown in Fig. 1 where good agreement is seen between experiment and the 3-band model.

More precise comparison with the calculated dispersion requires data for a single material at various wavelengths. Although all our DFWM data on semiconductors are for near bandgap ($\hbar\omega \approx E_g$) excitation, other experimental techniques can be used to further examine the theory. It can be shown that the A and B coefficients are proportional to the effective $\chi^{(3)}$ that is measured using a single beam with circular polarization. Therefore, simple experimental techniques such as Z-scan can be employed to determine the circular-to-linear dichroism

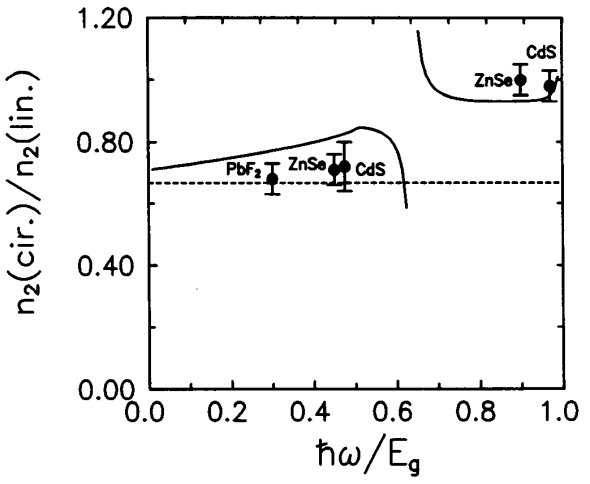

Fig. 2. The dispersion of the polarization dichroism of n_2 measured using Z-scan. The solid line is from the 3-band theory and the dashed line represents 2-band model [9]. The divergence near $\hbar\omega/E_g \cong 0.65$ corresponds to the zero-crossing of n_2 (linear polarization).

of $\chi^{(3)}$. With the Z-scan we can measure the real and imaginary parts of $\chi^{(3)}$ independently, which, in general, is not possible with DFWM. Specifically, the circular/linear ratio of the measured nonlinear refractive index coefficient n_2 ($\propto \Re e\{\chi^{(3)}\}$) is given by $2\Re e\{A\}/\Re e\{A+B+C\}$. It is worth noting that since we are dealing with normalized quantities, the absolute magnitudes of the nonlinear coefficients (that contain material dependent parameters such as band-gap energy and linear refractive index) are not involved.

We measured the n_2 dichroism for ZnSe and CdS at $\lambda = 1.064$ and 0.532 μm and PbF_2 at $\lambda = 0.532$ μm. The results are shown in Fig. 2 where good agreement with the calculated dispersion curve is seen. It is expected that at $\omega = 0$, $\chi^{(3)}$ must obey Kleinman symmetry making $\chi_{1221} = \chi_{1212} = \chi_{1122} = \chi_{1111}/3$, which in turn implies $A = B = C$. This symmetry also translates to an n_2 dichroism of 2/3 at $\omega = 0$. This occurs at the y-axis intercept of the dashed lines in Figs. 1 and 2. The simple 3-band model, while explaining the anomalous dispersion of the polarization dependent $\chi^{(3)}$ measurements, does not perfectly obey the Kleinman symmetry. A more rigorous theory, i.e., using a complete Kane 4-band model, and including the $\chi^{(3)}$ processes involving inter-valence band transitions should resolve this discrepancy.

In conclusion, we show that the anomalous dispersion of the polarization dependent DFWM and n_2 dichroism can be explained using a 3-band model. We find that, in deriving the symmetry properties of $\chi^{(3)}$, it is essential to consider the k-space orientation of the momentum matrix element with respect to the electrons quasi-momentum. We present experimental results for ZnSe, CdS, PbF_2, and NaCl that agree with the theory.

REFERENCES

[1] R. K. Jain and M. B. Klein, "Degenerate four-wave-mixing in semiconductors," in *Optical Phase Conjugation*, R. A. Fisher, Ed. New York: Academic, 1983, pp. 307–455.
[2] M. L. Claude, L. L. Chase, D. Hulin, and A. Mysyrowicz, *Optical Nonlinearities and Instabilities in Semiconductors*, H. Haug, Ed. New York: Academic, 1988, pp. 217–237.
[3] D. J. Hagan, H. A. MacKenzie, H. A. Al Attar, and W. J. Firth, "Carrier diffusion measurement in Insb by the angular dependence of DFWM," *Opt. Lett.*, vol. 10, pp. 187–189, 1985.
[4] E. J. Canto-Said, D. J. Hagan, J. Young, and E. W. VanStryland, "Degenerate four-wave-mixing measurements of high order nonlinearities in semiconductors," *IEEE J. Quantum Electron.*, vol. 27, pp. 2274–2280, 1991.
[5] A. L. Smirl, T. F. Boggess, B. S. Wherrett, G. Paul Perryman, and A. Miller, "Picosecond optically induced anisotropic state filling in semiconductors," *Phys. Rev. Lett.*, vol. 49, pp. 933–936, 1982.
[6] T. R. Rader and A. Gold, "Polarization dependence of two-photon absorption in solids," *Phys. Rev.*, vol. 171, pp. 997–1003, 1968.
[7] M. D. Dvorak, W. A. Schroeder, D. R. Anderson, A. L. Smirl, and B. S. Wherrett, "Measurement of the anisotropy of two-photon absorption coefficient in zincblende semiconductors," *IEEE J. Quantum Electron.*, vol. 30, p. 256, 1994.
[8] E. O. Kane, "Band-structure of indium antimonide," *J. Chem. Phys. Solids*, vol. 1, pp. 249–261, 1957.
[9] M. Sheik-Bahae, D. C. Hutchings, D. J. Hagan, and E. W. VanStryland, "Dispersion of bound-electronic nonlinear refraction in solids," *IEEE J. Quantum Electron*, vol. 27, pp. 1296–1309, 1991.
[10] M. Sheik-Bahae, J. Wang, and E. W. VanStryland, "Nondegenerate optical Kerr effect in semiconductors," *IEEE J. Quantum Electron.*, vol. 30, pp. 249–255, 1994.
[11] D. C. Hutchings and B. S. Wherrett, "Theory of anisotropy of two-photon absorption in zinc-blende semiconductors," *Opt. Mater.*, vol. 3, p. 53, 1994.
[12] M. Sheik-Bahae, A. A. Said, T. H. Wei, D. J. Hagan, and E. W. VanStryland, "Sensitive measurements of optical nonlinearities using a single beam," *IEEE J. Quantum Electron*, vol. 26, pp. 760–769, 1990.

M. Sheik-Bahae (M'87), photograph and biography not available at the time of publication.

J. Wang, photograph and biography not available at the time of publication.

E. J. Canto-Said, photograph and biography not available at the time of publication.

R. DeSalvo, photograph and biography not available at the time of publication.

D. J. Hagan (M'87), photograph and biography not available at the time of publication.

E. W. VanStryland (M'84–SM'90), photograph and biography not available at the time of publication.